THE JOURNAL OF COMPARATIVE NEUROLOGY 432:296–306 (2001)

Characterization of Neuropeptide Y–Expressing Cells in the Mouse Retina Using Immunohistochemical and Transgenic Techniques

JOHN ROBERT SINCLAIR AND SHEILA NIRENBERG*
Department of Neurobiology, University of California at Los Angeles (UCLA), Los Angeles, California 90095-1763

ABSTRACT

The amacrine cells of the retina are a complex family of interneurons. They are made up of numerous subgroups, each with different morphologic and/or biochemical properties and each presumably serving a different function. In this study, we characterized one subgroup, defined by its expression of a peptide, neuropeptide Y (NPY). The cells were identified using antibodies to NPY and characterized using a transgenic mouse line that expressed the reporter enzyme, β-galactosidase, in the NPY-immunoreactive (NPY-IR) cells. We found that NPY-IR cells were present in two layers, the inner nuclear layer (INL) and the ganglion cell layer (GCL). The cells in both layers were densely distributed, with those in the INL having a mean density of 1452 ± 65 cells/mm^2, and those in the GCL having a mean density of 644 ± 41 cells/mm^2. The cells in the INL extended their processes in the sublamina of the inner plexiform layer (IPL) closest to the INL/IPL border, the presumptive OFF sublamina, and the cells in the GCL extended their processes in the sublamina near the GCL/IPL border, the presumptive ON sublamina. Both populations of cells were immunoreactive to a GABA transporter and, thus, likely GABAergic. The high density of these cells suggests that they play a prominent role in IPL processing. The location of their processes suggests that one population acts in the pathway that mediates OFF responses, and the other in the pathway that mediates ON responses, and their expression of a GABA marker indicates that their actions are likely inhibitory. J. Comp. Neurol. 432:296–306, 2001.

Indexing terms: amacrine cells; GABA; immunohistochemistry; neuropeptides; mouse

Amacrine cells constitute a major class of interneurons in the retina. They lie in the inner nuclear layer (INL) and the ganglion cell layer (GCL) and are involved in the processing that occurs in the inner plexiform layer (IPL). One of the striking features of amacrine cells is their diversity—they do not form a single class but rather many subclasses (Perry and Walker, 1980; Kolb et al., 1981; Masland, 1988; Vaney, 1990; MacNeil and Masland, 1998). As many as 22 have been described, distinguished by differences in their morphologic and biochemical properties (Kolb et al., 1981; MacNeil and Masland, 1998).

The roles of most of these subclasses in IPL processing are not yet understood. Recent advances in transgenic techniques, such as cell ablation and gene inactivation, have opened the door to a variety of new tools for studying the actions of individual cell types, and these methods have already yielded new information about both IPL and outer plexiform layer (OPL) processing (Chen et al., 1995; Masu et al., 1995; Bonfanti et al., 1996; Nirenberg and Meister, 1997; Xu et al., 1997; Soucy et al., 1998; Lem et al., 1999; Toda et al., 1999; Yang et al., 1999; He et al., 2000).

Because these techniques are currently most feasible in the mouse, this species is becoming an attractive new model system for the study of retinal circuitry. Because the mouse retina has not yet been well-described anatomically, an important first step is to characterize its array of cell types. Recently, Jeon et al. (1998) made a significant

Grant sponsor: Whitehall Foundation; Grant sponsor: Klingenstein Fund.

*Correspondence to: Sheila Nirenberg, Department of Neurobiology, UCLA, 10833 Le Conte Avenue, Los Angeles, CA 90095-1763.
E-mail: sheilan@ucla.edu

Received 13 July 2000; Revised 18 December 2000; Accepted 27 December 2000

contribution by providing a description of the major cell classes and their relative proportions. The next step is to describe the subclasses. In this study, we characterize one subclass of putative amacrine cells, defined by its expression of a neuropeptide, NPY. This description enables predictions to be made about its actions in retinal circuitry, which can then be tested in subsequent studies using cell ablation and gene inactivation techniques.

MATERIALS AND METHODS

Experimental animals

Three sets of mice were used. The first was from a transgenic line generated in a C57BL/6J background that expressed the reporter gene *lacZ*, which encodes the enzyme β-galactosidase (β-gal), under the regulation of the NPY gene promoter. The mouse line was produced through homologous recombination by disrupting one NPY allele and replacing it with *lacZ* (Erickson et al., 1996). The second was from a transgenic line, also generated in a C57BL/6J background that expressed *lacZ* under the regulation of the Thy-1 gene promoter. This line was generated by inserting an exogenous vector containing a Thy-1 promoter linked to the *lacZ* gene (Kelley et al., 1994). The third set were nontransgenic animals of the C57BL/6J strain. All procedures on these animals were carried out under the regulation of the Animal Research Committee of the University of California at Los Angeles and in accordance with NIH guidelines.

Detecting β-gal expression by using 5-bromo-4-chloro-3-indolyl-D-galactopyranoside (Xgal)

To prepare Xgal-stained whole-mount retinas, we used the following procedure, modified from Cepko (1989): Animals were euthanized with CO_2, the eyes were removed, and the retinas were dissected in Liebovitz (L-15) medium (Sigma). The retinas were then laid flat on a glass coverslip and fixed in 0.5% glutaraldehyde in 0.1 M phosphate buffered saline (PBS), pH 7.4, for 5 minutes. The retinas were then transferred to a 24-well culture plate and fixed for an additional 10 minutes, washed three times in PBS, and incubated for >15 hours at 37°C or >36 hours at room temperature in Xgal reaction mix (0.8 mg/ml Xgal in 35 mM potassium ferrocyanide, 2 mM $MgCl_2$, 0.02% Nonidet P-40, and 0.01% sodium deoxycholate in PBS, pH 7.4). Finally, the retinas were washed three times in PBS and mounted on "tunnel" slides, which contain a recessed area in the center to hold tissue. With a tunnel slide, a coverslip can be placed over the slide without compressing the tissue.

To maintain the orientation of each retina as a whole-mount, the eye was marked before removal from the euthanized animal. A hot probe was placed briefly against the superior cornea, marking it with a white spot (0.5 mm). The eye was then removed, and a small incision was made into the retina at the location of the spot, producing a landmark.

To prepare Xgal stained cross-sections, animals were anesthetized with Nembutal (1 mg/kg), then perfused through the heart with 50 ml of PBS, pH 7.4, followed by 200 ml of 0.5% glutaraldehyde or 4% paraformaldehyde in PBS. The eyes were removed and post-fixed in the same fixative for 1 hour, hemisected, post-fixed further for 30 minutes and washed three times in PBS. The retinas were stained with Xgal as above for the whole-mounts, washed three times in PBS, followed by cryoprotection in 30% sucrose in PBS. The retinas were embedded in tissue freezing medium and cut on a cryostat. Sections were mounted on slides coated with gelatin or poly-L-lysine (0.01% w/v) and stored at −20°C until used for immunohistochemistry.

Immunohistochemistry

NPY immunohistochemistry was carried out by using an affinity-purified rabbit polyclonal antibody raised against NPY (Ab# 8711, generously provided by J.H. Walsh and H. Wong of the University of California at Los Angeles). Retinas were prepared by perfusing the animals with 50 ml of PBS, pH 7.4, followed by 4% paraformaldehyde (when fluorescence immunohistochemistry was used) or 0.5% glutaraldehyde (when avidin-biotin-peroxidase immunohistochemistry was used). The eyes were removed and post-fixed in the same fixative for 1 hour, hemisected, post-fixed further for 30 minutes, washed three times in PBS, cryoprotected in 30% sucrose overnight, embedded in tissue freezing medium, and cryostat sectioned onto gelatin or poly-L-lysine (0.01% w/v) −coated slides. Sections were fixed to the slides with the same fixative used for the perfusion, washed three times in PBS, treated with 3% H_2O_2 for 30 minutes to quench endogenous peroxidase activity, and washed again three times in PBS. For glutaraldehyde-fixed tissue, sections were also washed once in distilled water (dH_2O) and treated with 0.1 M sodium borohydride, then washed three times in dH_2O, and once in PBS. The sodium borohydride treatment was found to be essential for NPY antibody penetration into sections. Retinas were then incubated in blocking solution (10% goat serum with 0.5% Triton-X in PBS) for 1 hour at room temperature or overnight at 4°C followed by an overnight incubation at 4°C in NPY antibody in blocking solution. The NPY antibody was diluted 1:2,000 when a fluorescent secondary antibody was used and 1:8,000 when the avidin-biotin peroxidase method (Vectastain ABC kit, Vector Labs) was used. After incubation with NPY antibody, sections were washed at least three times in PBS and then incubated at room temperature for 2 hours in Rhodamine Red X secondary antibody (Jackson ImmunoResearch Laboratories) at a dilution of 1:800 or a biotinylated secondary antibody (Vectastain ABC kit) at a dilution of 1:200 in a 1:2 dilution of blocking solution. Sections stained with Rhodamine Red X were washed in at least three changes of PBS and cover-slipped in 2% potassium iodide in a 90% glycerol solution in PBS. Sections stained with the biotinylated secondary antibody were washed in at least three changes of PBS, then incubated in the Vectastain avidin-biotin-complex (ABC) for 1 hour at room temperature, then washed again three times in PBS, and reacted with 3,3′-diaminobenzidine (DAB) and H_2O_2 (DAB staining kit, Vector Laboratories). Finally, the slides were cover-slipped in Gel/Mount media (Biomeda Corp).

The specificity of the NPY antibody was determined by pretreating it with synthetic NPY (10 μM) (Bachem Chemicals) and staining sections as described above. As expected, sections stained with pretreated NPY antibody showed no cell body labeling (compare Fig. 1A with B).

GAT-1 staining (Brecha and Weigmann, 1994) was carried out by using a polyclonal antibody raised against the GABA transporter, GAT-1 (Chemicon International), diluted 1:200. All staining was carried out in sections fixed

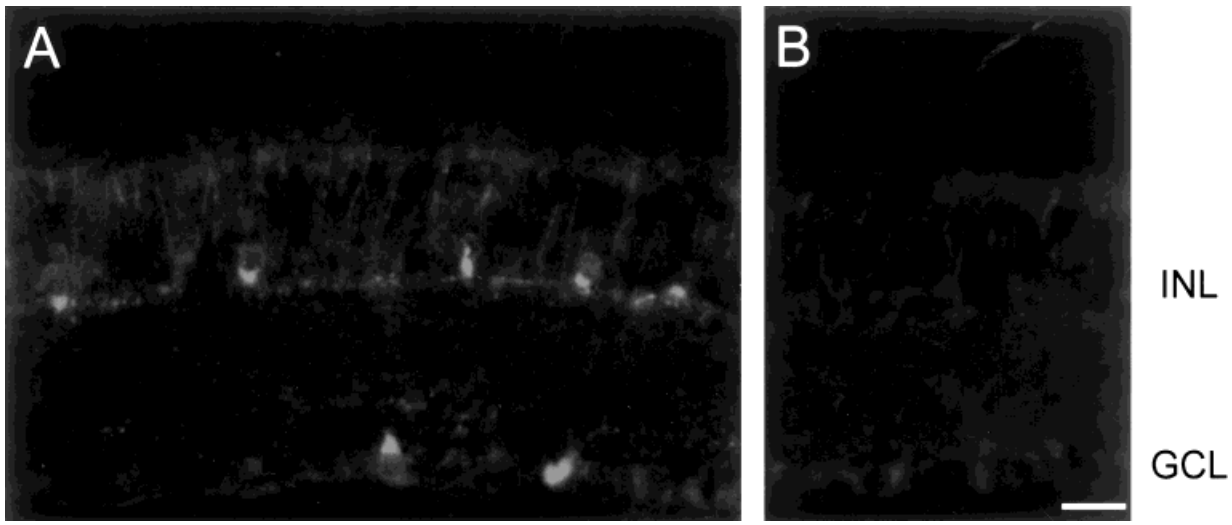

Fig. 1. Neuropeptide Y (NPY) immunoreactivity in the retina. **A:** Retinal cross-section (10 μm) stained with NPY antibody. **B:** Cross-section (10 μm) stained with NPY antibody that had been pretreated with excess synthetic NPY. INL, inner nuclear layer; GCL, ganglion cell layer. Scale bar = 20 μm.

with 4% paraformaldehyde by using the Rhodamine Red X secondary antibody as described above.

Testing for colocalization of Xgal and antibodies to NPY or GAT-1

For sections stained with a fluorescent antibody, the following procedure was used: Each section was digitally imaged first under brightfield illumination to visualize the Xgal-stained cells and then under epifluorescence to visualize the antibody-stained cells (either NPY or GAT-1). A transparency was then placed over the brightfield image, and each Xgal-stained cell was marked in red. The transparency was then placed over the fluorescence image, and all immunoreactive cells were marked in green. The transparency was then examined for the number of red and green marks that overlapped, the number of red marks without green overlap, and the number of green marks without red overlap. For sections stained with the avidin/biotin peroxidase method, the procedure was slightly different. Sections were first stained with Xgal as described above and then digitally imaged. The imaging was done by using a water immersion objective that was placed in direct contact with the fluid above the section. This procedure was necessary because the slides were subsequently immunostained and, therefore, could not be cover-slipped. The sections were then stained with an antibody to either NPY or GAT-1, and the identical section was then imaged. Colocalization was then assessed by using a transparency as described above.

Labeling ganglion cells with DiI and β-gal expressing cells with fluorescein

To determine whether NPY/β-gal cells in the GCL were ganglion cells or displaced amacrine cells, retinas were treated with two dyes, one for marking ganglion cells and one for marking β-gal–expressing cells, and the extent of colocalization was assessed. To mark ganglion cells, the carbocyanin dye DiI was used; for marking β-gal–expressing cells, the β-gal substrate fluorescein-di-β-D-galactopyranoside (FDG) was used. FDG releases fluorescein when hydrolyzed by β-gal.

Ganglion cells were labeled with DiI (Molecular Probes) by injecting 10 μl of 20 mg/ml DiI in dimethyl sulfoxide into the superior colliculus of the anesthetized mouse. Hofbauer and Drager (1985) reported that the superior colliculus receives afferents from most or all ganglion cells in the mouse retina. The dye was allowed 3 days for retrograde transport to the retina. The retina was then removed from the animal, dissected into several pieces in L-15 media, and treated with FDG (Molecular Probes). Specifically, each piece was removed from the dissecting dish and placed on a glass slide ganglion cell side up. The L-15 was then removed and replaced with FDG solution (10 μl of 3.75 mM FDG in 2.5% dimethyl sulfoxide/97.5% L-15). The tissue was then transferred to a tunnel slide and imaged under fluorescence optics by using a Texas Red filter to see the DiI and a fluorescein isothiocyanate filter to see the fluorescein. (See above for description of tunnel slide.) Only retinas that showed a high degree of DiI-labeling were used.

Determining the probability that a cell *not* labeled with DiI is *not* a ganglion cell

Because DiI injected into the SC may not label all ganglion cells, one cannot assume that the lack of DiI labeling in a cell in the GCL means that it is not a ganglion cell. To determine the probability that a cell in the GCL is not a ganglion cell given that it lacked DiI-labeling, we used Bayes' theorem, which gives

$$P(\text{not GC} \mid \text{not labeled}) = \frac{P(\text{not labeled}|\text{notGC})P(\text{not GC})}{P(\text{not labeled})}$$

where $P(\text{not GC} \mid \text{not labeled})$ is the probability that a cell in the GCL was not a ganglion cell given that it lacked DiI labeling, $P(\text{not labeled} \mid \text{not GC})$ is the probability that a

cell in the GCL lacked DiI-labeling given that it was not a ganglion cell, P(not GC) is the probability that a cell in the GCL was not a ganglion cell, and P(not labeled) is the probability that a cell in the GCL lacked DiI labeling. Because a cell cannot be labeled with DiI if it is not a ganglion cell, P(not labeled | not GC) = 1, and we need only to determine P(not GC) and P(not labeled).

To determine P(not labeled), the probability that a cell in the GCL lacked DiI labeling, we measured the density of DiI-labeled cells in seven sampling areas (466 × 364 μm, from midperipheral retina) and found a density of 3,850 ± 321 cells/mm^2. We then measured the total density of cells in the GCL, also by using seven sampling areas from midperipheral retina and found a density of 9430 ± 483 cells/mm^2. For the latter, retinas were fixed and stained with ethidium homodimer to mark cell nuclei, following the method of Jeon et al. (1998). Cell density was measured correcting for tissue shrinkage due to the fixation. Dividing the mean density of DiI-labeled cells by the mean density of all cells in the GCL gave the probability that a cell in the GCL was labeled with DiI; this probability was 0.41. The probability that a cell in the GCL lacked DiI labeling was, thus, 0.59. To determine the probability that a cell in the GCL was not a ganglion cell, P(not GC), we used the previously measured value of 0.55, made by Jeon et al., (1998) by using electron microscopic analysis. Dividing 0.55 by 0.59, we find that P(not GC | not labeled), the probability that a cell in the GCL that lacked DiI labeling was not a ganglion cell, was 0.93.

Density analysis

Whole-mount retinas were prepared and stained with Xgal as described above to calculate the density of NPY/β-gal cells across the retina. Images were acquired from 466 × 364 μm areas along the superior-inferior axis and nasal-temporal axis, and all Xgal-labeled cells within each area were counted.

Nearest neighbor analysis

Regularity of the distribution of the NPY/β-gal cells was measured using nearest neighbor analysis in Xgal-labeled whole-mounts (Clark and Evans, 1954; Wassle and Riemann, 1978). In each quadrant of the whole-mount, a region (466 × 364 μm) was digitally imaged. The (x, y) coordinates of all cells in each region were recorded, and their nearest neighbor distances were measured. The distribution of nearest neighbor distances was then compared with the distribution associated with a random population. The random population was constructed so that it had the same cell density as the experimentally observed population, with the added constraint that the cells could not be closer than one cell body diameter. This constraint was used because the cells in a given layer did not show overlap — that is, the NPY/β-gal cells in the INL were in a single layer (the innermost row); similarly, the NPY/β-gal cells in the GCL were in a single layer (e.g., see Fig. 4C). As shown by Wassle and Riemann (1978), the probability distribution of nearest neighbor distances for nonoverlapping cells, $P(d)$, is given by

$$P(d) = 2\pi d\lambda^* \exp[-\pi(d^2 - d_c^2)\lambda^*], \quad (1)$$

where d_c is the cell body size, and λ^* is the effective cell density (see Wassle and Riemann (1978) for detailed discussion), related to the true cell density, λ, by

$$\lambda = \lambda^* \exp(-\pi d_c^2 \lambda^*),$$

Because d_c is the smallest possible nearest neighbor distance, $P(d) = 0$, when $d < d_c$.

For each quadrant in the retina, the distribution of nearest neighbor distances was compared, by using the Kolmogorov-Smirnov test, to those from the relevant random distribution given in Eq. (1).

Confocal imaging of the processes of NPY/β-gal cells

Retinas were dissected in L-15 into small pieces (typically 1.5 × 1.5 mm), stained with FDG, and placed on ice for 15–30 minutes. Each retina was then transferred to a tunnel slide, immersed in a solution of 1% potassium iodide in 45% glycerol in L-15 to reduce photobleaching, and covered with a coverslip. The retina was recessed in the tunnel slide, so the coverslip did not compress it. The retina was then optically sectioned by using a Zeiss laser scanning confocal microscope (LSM 410, Zeiss Instruments) from the fiber layer to the middle of the INL in steps of 0.5 μm. Images were obtained with 40× Zeiss FLUAR oil immersion objective by using an FITC bandpass filter (515–540 nm). Well-labeled NPY/β-gal cells were identified, and the location of their processes was determined by measuring the distance from the GCL/IPL border normalized to the width of the IPL. All cells examined were unistratified, allowing a single number to be assigned to each cell.

Digital image generation

All images were generated by using a digital camera. Scaling, contrast, and brightness adjustment were carried out in Adobe Photoshop 5.0 (Adobe Systems).

RESULTS

Identification of NPY-IR cells

NPY-IR cells were found almost exclusively in two layers: the GCL and the innermost row of the INL (Fig. 1A). Occasional cells were found in the outermost row of the INL, but these constituted fewer than 3% of the total NPY-IR population. The immunoreactive staining was eliminated by pretreating the antiserum with excess synthetic NPY, indicating that the antibodies were specific for the peptide (Fig. 1B).

Using β-galactosidase as a marker for NPY-IR cells

The NPY immunostaining in the mouse retina was punctate, both in the cell bodies and the processes, and was not ideal for extensive characterization of the cells. For more detailed analysis, we used a transgenic mouse line that expressed the gene for the enzyme β-galactosidase (β-gal) in the NPY-IR cells. This line, produced by Erickson et al. (1996), expressed β-gal under the regulation of the NPY gene promoter. It was generated by homologous recombination, whereby one allele at the NPY locus was replaced by the gene for β-gal. The animals in this line were heterozygous for both genes and phenotypically were normal (Erickson et al., 1996).

With this mouse line, NPY-expressing cells could be stained not just with NPY antibodies, but with substrates for β-gal, which provide stronger signals. In particular, 5-bromo-4-chloro-3-indolyl-D-galactopyranoside (Xgal) could

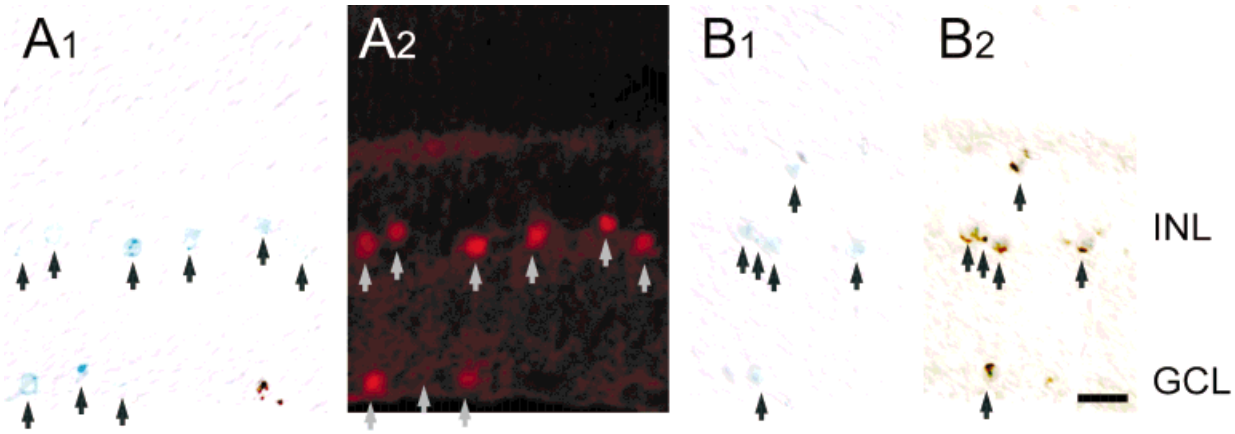

Fig. 2. Colocalization of Xgal and neuropeptide Y (NPY) immunostaining. **A_1:** Retinal cross-section (10 μm) stained with Xgal to mark β-gal-expressing cells. Xgal forms a blue precipitate in the cell bodies (arrows). **A_2:** Same section stained with NPY antibody. Arrows indicate the positions of the Xgal-stained cells. **B_1:** A different section stained with Xgal. Arrows indicate Xgal-stained cells. **B_2:** Same section as B_1 stained with antibody to NPY, this time by using the avidin-biotin peroxidase method for antibody detection. Arrows indicate same cells as in B_1. INL, inner nuclear layer; GCL, ganglion cell layer. Scale bar = 20 μm in B_2 (applies to A_1–B_2).

be used as a marker of NPY-expressing cell bodies in whole-mounts, because it produces a dark precipitate in β-gal–expressing cells, and fluorescein-di-β-D-galactopyranoside (FDG) could be used to assess NPY-expressing cell processes, because it produces a diffusible fluorescent product (fluorescein) that fills cell processes.

To use this mouse line, it was first necessary to verify that the β-gal enzyme was correctly expressed in the NPY-IR cells. To address this, retinas were double stained with NPY antibody and the β-gal substrate Xgal (Fig. 2). Forty sampling areas from three retinas were assessed, and all Xgal-stained and NPY-IR cells in each were counted. First, Xgal-stained cells were examined for the presence of NPY immunostaining. Ninety-four percent of Xgal-stained cells showed NPY immunostaining (297 of 314 Xgal-stained cells in the INL and 125 of 134 in the GCL). Second, NPY-IR cells were examined for the presence of Xgal staining. Eighty-five percent of NPY-IR cells showed Xgal staining (297 of 339 NPY-IR cells in the INL and 125 of 156 cells in the GCL). This high degree of colocalization indicated that β-gal expression in this transgenic line would serve as a reliable marker for NPY immunoreactivity. β-gal–expressing cells in this line, thus, are referred to as NPY/β-gal cells.

Determining whether NPY cells in the GCL are amacrine or ganglion cells

As shown in Figures 1 and 2, NPY/β-gal cells (or NPY-IR cells) are present in two layers, the INL and GCL, raising the question of whether they are all amacrine cells. Specifically, are those in the GCL amacrine or ganglion cells? To assess this question, ganglion cells were labeled with one dye, the carbocyanin dye DiI, and NPY/β-gal cells were labeled with a different dye, fluorescein, and the retina was examined for dye colocalization (Fig. 3A–C) (see Materials and Methods section). The number of fluorescein-labeled cells that showed DiI was then counted. Fewer than 10% of fluorescein-labeled cells showed DiI labeling (10 of 107 cells examined, 3 retinas, 7 sampling areas). The occasional double-labeling may have been the result of overlap between fluorescein-labeled cells and DiI-labeled cells, because cells in the GCL of the mouse retina are tightly packed.

As an additional check that colocalization of the fluorescein and DiI would have been clearly visible had it occurred, we performed the following positive control: Ganglion cells were labeled with DiI in a transgenic mouse line that expressed β-gal specifically in ganglion cells. In this line, β-gal is expressed under the regulation of the Thy-1 gene promoter (Kelley et al., 1994), which is active in a large subset of ganglion cells. We then performed the identical experiment as above. Because the β-gal–expressing cells in this line were ganglion cells, the expected result was that all fluorescein-labeled cells would show DiI. As expected, >90% of the fluorescein-labeled cells showed DiI labeling (178 of 196 cells, 2 retinas, 6 sampling areas) (Fig. 3D,E,F).

In summary, the lack of DiI in >90% NPY/β-gal cells and the clear presence of DiI in >90% of Thy-1/β-gal cells provides strong indication that the NPY cells in the GCL are not ganglion cells. Note, though, that the lack of DiI in a given cell in the GCL cannot ensure that it is not a ganglion cell, because the labeling of ganglion cells with DiI was short of complete. Thus, we can only assign a probability that a given unlabeled cell in the GCL is not a ganglion cell, which we estimate to be 93% (see Materials and Methods section). Thus, the DiI assay only allows us to assert with confidence that >84% of the NPY–β-gal cells are not ganglion cells (93% of the 90% not labeled with DiI).

Distribution of NPY cells in the GCL and INL

The density and distribution of NPY/β-gal cells was examined in retinal whole-mounts using the β-gal substrate Xgal. As mentioned above, Xgal forms a blue precipitate in the cell bodies, providing a strong signal for NPY/β-gal cells and allowing those below the surface to be clearly visualized (Fig. 4). The mean density of NPY/β-gal cells, averaged over six retinas, was 1,452 ± 65 cells/mm^2 (SEM, n = 6) in the INL and 644 ± 41 cells/mm^2 (SEM, n = 6) in the GCL (Fig. 5); thus, on average, the density in

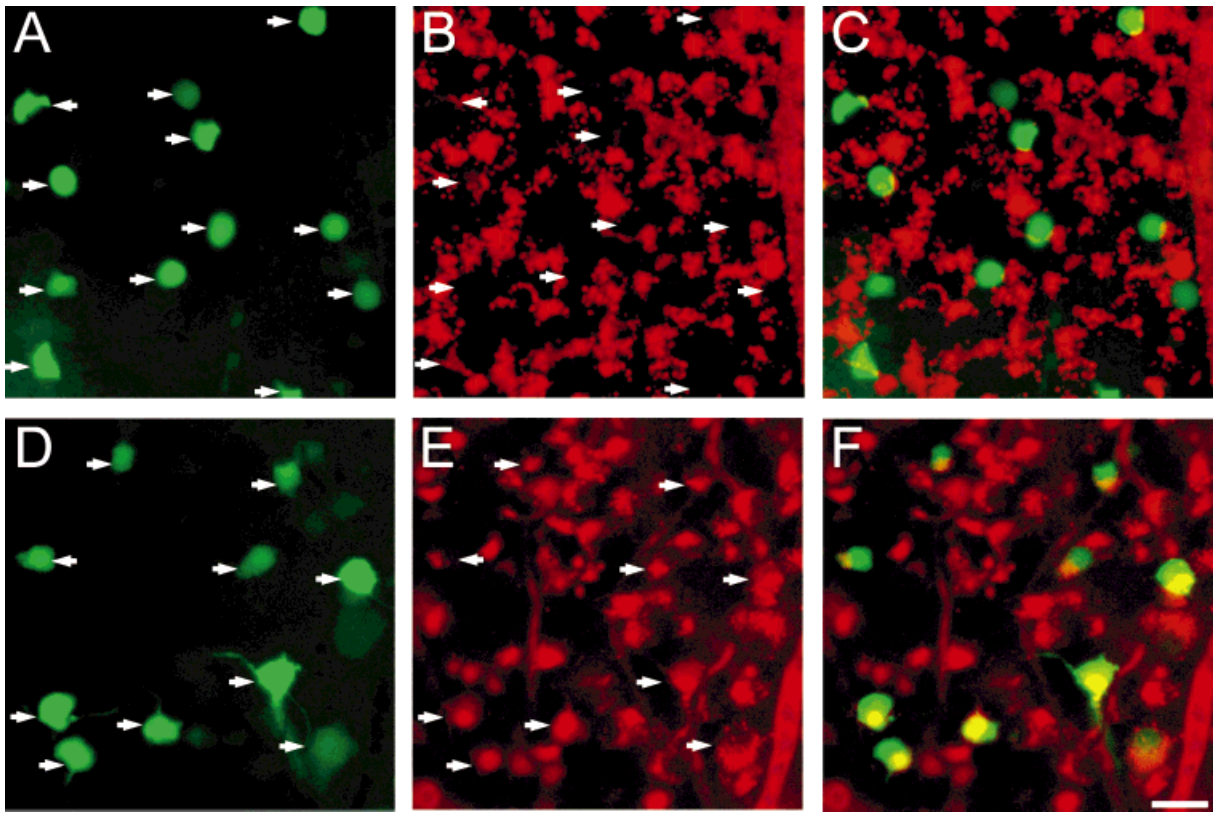

Fig. 3. Fewer than 10% of neuropeptide Y (NPY)/β-gal cells in the ganglion cell layer (GCL) show labeling with DiI, indicating that they are not ganglion cells. Top: Live retinal whole-mount labeled with fluorescein (green) to mark the NPY/β-gal cells and DiI (red) to mark the ganglion cells. **A:** View through the fluorescein filter, which shows only the fluorescein-labeled cells. **B:** View though the rhodamine filter, which shows only the DiI-labeled cells. Arrows indicate the locations of all the fluorescein labeled cells. **C:** The two pictures superimposed. Yellow indicates overlap. Bottom: Whole-mount from a Thy-1/β-gal mouse, which expresses β-gal in a subset of ganglion cells. In this mouse line, the β-gal marker, fluorescein, would be expected to colocalize with the ganglion cell marker, DiI. **D:** View through the fluorescein filter, which shows only the fluorescein-labeled cells. **E:** View though the rhodamine filter, which shows only the DiI-labeled cells. **F:** The two pictures superimposed. Yellow indicates overlap. Scale bar = 20 μm in F (applies to A–F).

the INL is just over twice that in the GCL. Note that nearly all cells in the INL lie in the innermost row (596 of 623 examined, 96%) (see Fig. 4C). The density of NPY/β-gal cells is slightly lower in peripheral retina than in central retina in the nasal and superior quadrants in both the INL and GCL ($P < 0.05$, Student's t-test) but is not significantly lower in the temporal or inferior quadrants ($P > 0.05$).

To determine whether the NPY/β-gal cells cover the retinal surface in a regular manner, we performed nearest neighbor analysis (Clark and Evans, 1954; Wassle and Riemann, 1978), which measures the intercell distances in the population. Although a more direct way to assess whether NPY/β-gal cells cover the retinal surface is to assess coverage by the cells' processes, neither the Xgal stain nor the NPY antiserum adequately labeled processes, precluding the possibility of this test. Thus, nearest neighbor analysis was used as a first approximation of retinal coverage.

The analysis was performed in each of four quadrants: superior, inferior, nasal, and temporal (Fig. 6). In each quadrant, the nearest neighbor distances were determined, and the distribution of distances was then compared with the distribution produced by random placement of cells, using the same cell density (see Materials and Methods section). In all quadrants examined in both the GCL and INL for three retinas, the distribution of nearest neighbor distances was found to be significantly different from that produced by random cell placement ($P < 0.002$, Kolmogorov-Smirnov test).

The degree of regularity was then measured by using a regularity index (RI), which is the mean nearest neighbor distance divided by the standard deviation. Higher RI values indicate more regular spacing. The values for NPY/β-gal cells ranged from 2.1–2.6 in the GCL and 2.6–3.0 in the INL. For comparison with other well-described cell types, the RI for NPY/β-gal is close to that of the S2 type serotonin-accumulating neurons in rabbit retina (RI = 2.8) (Sandell and Masland, 1986) but is considerably lower than that of the cholinergic neurons in the peripheral INL of the rabbit retina (RI = 5.9) (Vaney et al., 1981; Vaney, 1990). Thus, although the spacing of the NPY/β-gal cells is clearly not random, it is not highly regular.

Locations of the processes of NPY cells in the IPL

The location of the processes of individual NPY/β-gal cells were examined using FDG. Live whole-mount retinas

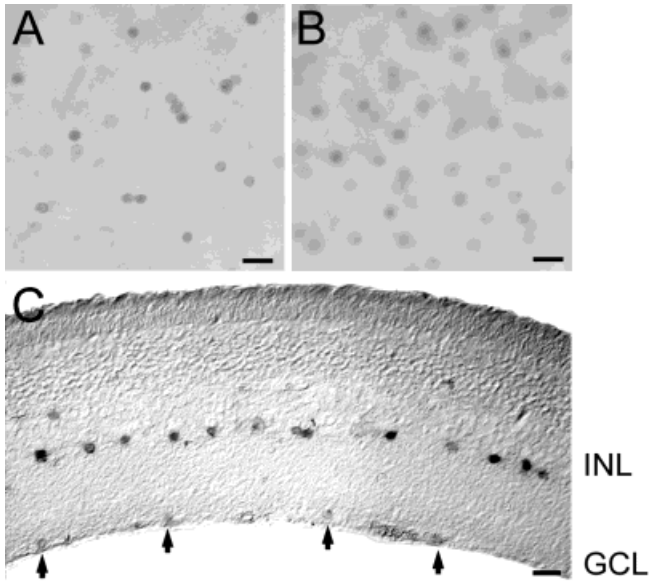

Fig. 4. Neuropeptide Y (NPY)/β-gal cells can be easily visualized in the ganglion cell layer (GCL) and inner nuclear layer (INL) using Xgal, which forms a blue precipitate. **A:** View of whole-mount retina stained with Xgal to mark the NPY/β-gal cells, focused on the GCL. **B:** View of the same retina, but focused on the INL. **C:** Retinal cross-section (25 μm), showing NPY/β-gal cells in the INL and GCL. Scale bars = 20 μm.

were treated with FDG to label the NPY/β-gal cells with fluorescein (Fig. 7A). The retinas were then placed in a tunnel slide and serial sectioned from the fiber layer through the middle of the INL with confocal microscopy. The processes of 25 cells were examined, 12 of which were from the INL and 13 of which were from the GCL. Only cells whose processes were visible for a length greater than the width of the IPL were examined. The results showed that NPY/β-gal cells in the INL were unistratified, with all showing ramifications in the outer third of the IPL. The mean normalized distance from the GCL/IPL border was 0.80 ± 0.02 (SEM, n = 12). NPY/β-gal cells in the GCL were also unistratified and ramified in the inner third of the IPL. The mean normalized distance from the GCL/IPL border was 0.28 ± 0.02 (SEM, n = 13) (Fig. 7B,C). The mean normalized distances for the two populations were statistically significantly different ($P < 0.0001$, Student's t-test). Thus, NPY/β-gal cells seem to comprise two groups, distinguished by the different locations of their processes in the IPL.

Analysis of NPY/β-gal cell processes also showed that the cells in the GCL clearly lack axons, as no projections to the fiber layer were observed (0 of 13 cells examined). This finding provides further evidence that the NPY/β-gal cells in the GCL are not ganglion cells but amacrine cells.

Expression of the GABA transporter GAT-1 in NPY cells

Previous studies have reported that NPY is colocalized with GABA, both in the retina (Main et al., 1993) and in other brain areas (McDonald and Pearson, 1989). To investigate whether NPY/β-gal cells in the mouse retina are likely GABAergic, retinas were double stained with antibodies to a GABA marker, the GABA transporter GAT-1, and with Xgal. Colocalization of the two stains was then determined (Fig. 8). Ninety-seven percent of NPY/β-gal cells examined (72 of 74 cells, 3 retinas, 23 sampling areas) showed clear GAT-1 labeling. The presence of GAT-1 immunoreactivity in NPY/β-gal cells in both the INL and GCL provides strong indication that these cells are inhibitory and use GABA as a transmitter. It also adds strong additional evidence that the NPY/β-gal cells in the GCL are not ganglion cells, because it has been shown previously by others that the presence of a GABA marker is inconsistent with their being ganglion cells (Cardozo et al., 1991).

DISCUSSION

We have examined NPY-expressing cells in the mouse retina and found the following: (1) They lie almost exclusively in two layers, i.e., the GCL and the innermost row of the INL. Occasional cells are present in the outermost row of the INL, but these constitute fewer than 3% of the total NPY-expressing population and are likely displaced cells. (2) The cells in both the INL and GCL are likely amacrine cells. The evidence that the cells in the GCL are amacrine cells is threefold. First, the vast majority cannot be backlabeled by injection of DiI into the superior colliculus. Second, they do not show the presence of an axon when their processes are labeled with FDG. Third, they show immunoreactivity to GAT-1, a GABA transporter, indicating that they are likely inhibitory neurons. (3) The processes of the NPY cells in the INL terminate in the sublamina closest to the border of the INL and IPL, whereas the processes of the cells in the GCL terminate near the GCL/IPL border. (4) NPY cells in both the INL and GCL are densely distributed, with those in the INL having a mean density of 1452 ± 65 cells/mm^2 and those in the GCL having a mean density of 644 ± 41 cells/mm^2. For comparison, these densities are close to that of the cholinergic cells and within a factor of 5 of ganglion cells. The mean density of cholinergic cells in the mouse retina is 1,100 cells/mm^2 in the INL and 945 cells/mm^2 in the GCL; the mean density of ganglion cells in the mouse retina is 3,300 cells/mm^2 (Jeon et al., 1998). (5) The intercell spacing of NPY-cells is nonrandom. The regularity index (RI) for NPY cells ranged from 2.1–2.6 in the GCL and 2.6–3.0 in the INL. For comparison, these values are close to that measured for the S2-type serotonin-accumulating neurons in rabbit retina (RI = 2.8) (Sandell and Masland, 1986) but are lower than that of the cholinergic cells in the INL rabbit retina (RI = 5.9) (Vaney et al., 1981; Vaney, 1990). Note that the measurements of intercell spacing were made treating the cells in each layer as a single population. It is possible that the cells in each layer form more than one mosaic. This might explain why some NPY cells are close to each other or even touching (see Fig. 6).

These findings enable general predictions to be made about the roles of NPY cells in retinal processing. First, the fact that they are amacrine cells and not ganglion cells indicates that they are interneurons rather than projection neurons and, thus, participate in processing within the retina, rather than transmitting information from the retina to higher brain areas. Second, their ramifications indicate that they are not a homogeneous population, but rather constitute two different (or symmetric) populations, i.e., one that lies in the INL and likely acts in the OFF pathway and one that lies in the GCL and likely acts in the ON pathway. Third, their expression of a

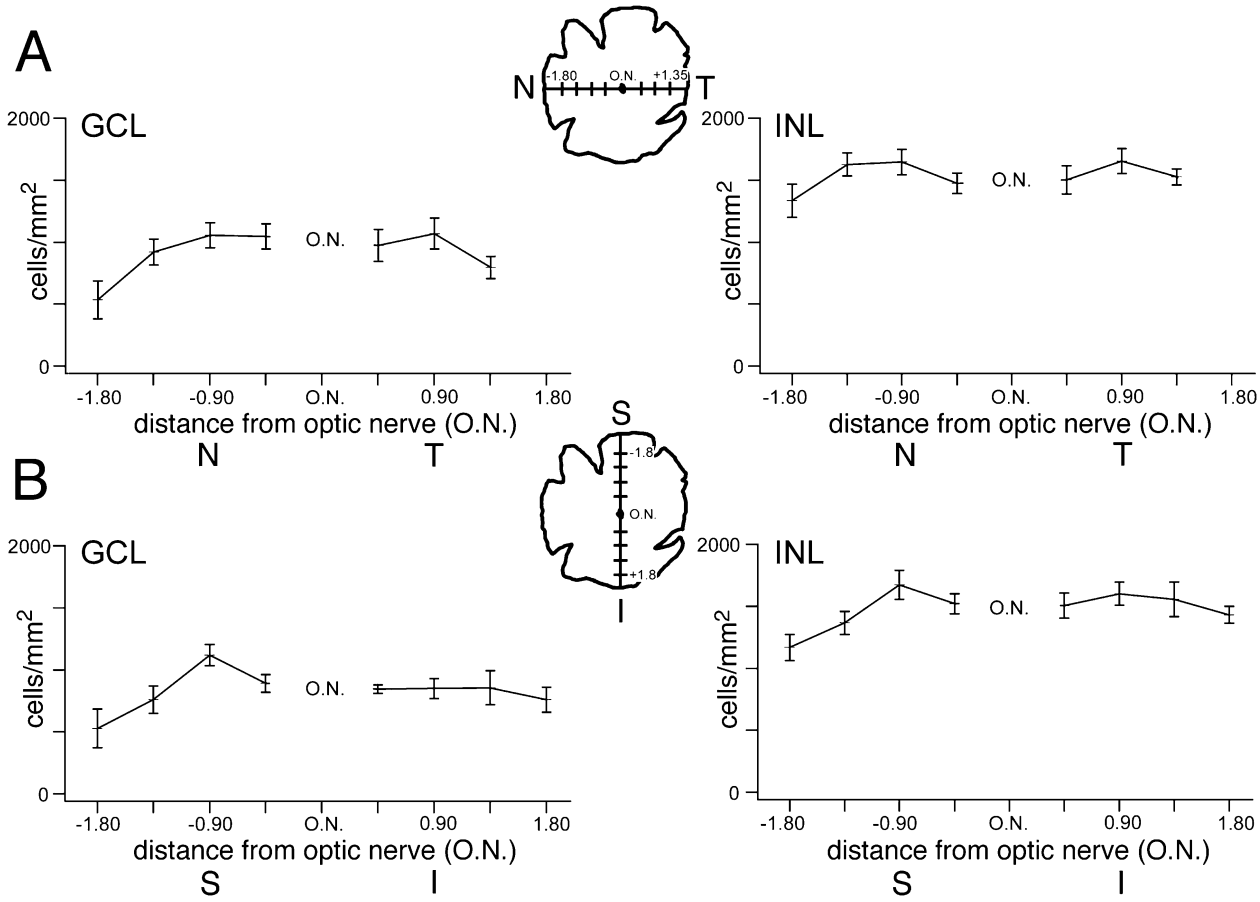

Fig. 5. Neuropeptide Y (NPY)/β-gal cell density from central to peripheral retina. **A:** Density along the nasotemporal axis (N, T) for NPY/β-gal cells in the ganglion cell layer (GCL) and inner nuclear layer (INL). **B:** Density along the superior/inferior axis (S, I) for NPY/β-gal cells in the GCL and INL. All density measurements were averaged over six retinas.

GABA marker suggests that their roles in these pathways are inhibitory. Finally, their high density suggests that they play a prominent role in these pathways. These predictions can be tested by ablating the NPY cell populations and examining the effects on the response properties of the retinal output neurons, the ganglion cells.

Using transgenic techniques to characterize NPY cells

To characterize NPY cells, we used a transgenic approach in addition to immunohistochemical methods. The transgenic approach was used because NPY immunostaining in the mouse retina was punctate in both the cell bodies and dendrites and limited our ability to analyze the cells' properties. The method was to use a mouse line that expressed the gene for the enzyme β-gal under the regulation of the NPY gene promoter. With this line, substrates for β-gal, which provide stronger stains than NPY antibodies, could be used to label the NPY cells. In particular, Xgal, which produces a dark precipitate in the cells, was used to label NPY cell bodies in whole-mounts, and FDG, which produces a diffusible fluorescent product (fluorescein), was used to reveal cell processes.

The immunohistochemical and transgenic approaches produced very similar but not identical results. Virtually all (94%) of the β-gal expressing cells examined were NPY immunoreactive. Thus, properties observed about the β-gal–expressing cells can be directly attributed to the NPY cells. However, not all (85%) NPY-IR cells were β-gal expressing. This presumably occurred because the β-gal substrate Xgal was a less sensitive assay for NPY cells than NPY antibodies. Thus, estimates of the density of NPY cells using Xgal are slight underestimates, and estimates of nearest neighbor distances are slight overestimates.

Comparison with other species

NPY immunoreactivity has been observed in the retinas of several mammals, including human (Tornqvist and Ehinger, 1988; Straznicky and Hiscock, 1989), cat (Hutsler et al., 1993; Hutsler and Chalupa, 1994), guinea pig (Bruun et al., 1986), monkey (Marshak, 1989), baboon (Bruun et al., 1986), and rat (Ferriero and Sagar, 1989). Although the staining patterns vary, they all have one feature in common: staining in the innermost row of the INL and in the first sublamina of the IPL, the presumptive OFF sublamina (Famiglietti and Kolb, 1976; Nelson et al., 1978; Peichl and Wassle, 1981). The different species vary in the other NPY-IR cells they contain, such as populations in the proximal INL and in the GCL. The most striking variation is found in cat, where

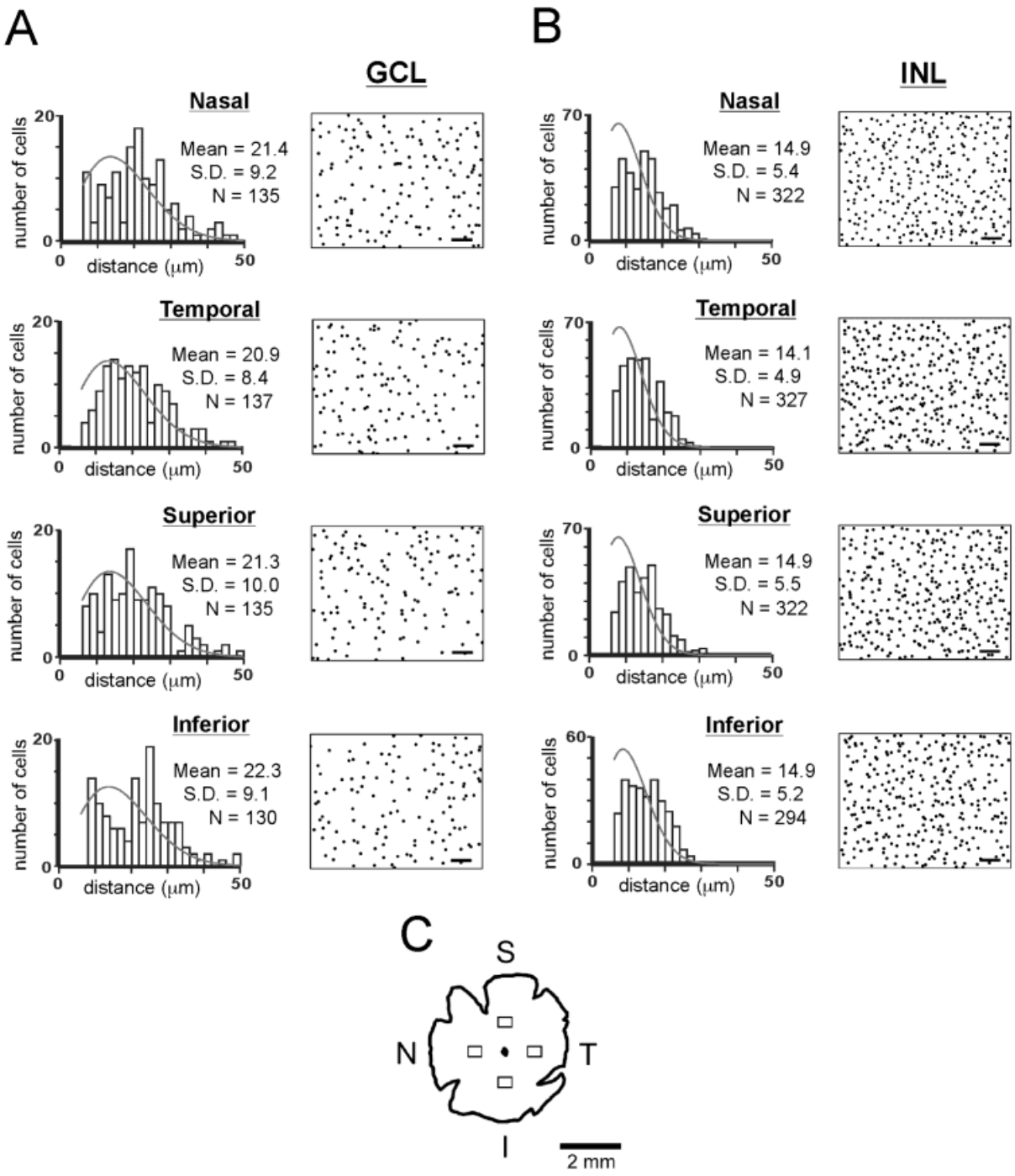

Fig. 6. Neuropeptide Y (NPY)/β-gal cells are not randomly distributed. Nearest neighbor analysis was performed in the four retinal quadrants (nasal, temporal, superior, and inferior) in the ganglion cell layer (GCL; **A**), and the inner nuclear layer (INL; **B**). Each plot shows the distribution of nearest neighbor distances of the NPY/β-gal cells in the quadrant examined (bars) and the distribution of nearest neighbor distances produced by random placement of cells, using the same cell density (see Materials and Methods section) (solid line). A digitized representation of the NPY/β-gal cells in each quadrant is adjacent to each plot. **C:** Location of the sampling area in each quadrant. N, nasal; S, superior; T, temporal; I, inferior. Scale bars = 50 μm in A,B.

NPY-IR cells in the GCL are not amacrine cells but ganglion cells (Hutsler et al., 1993).

Thus, our findings in mouse are in general agreement with those reported for other species in that the main population of NPY-IR cells lies in the innermost row of the INL and projects to the sublamina closest to the INL/IPL border. With regard to the second population of NPY-IR cells, our findings agree with descriptions in rat, which show that

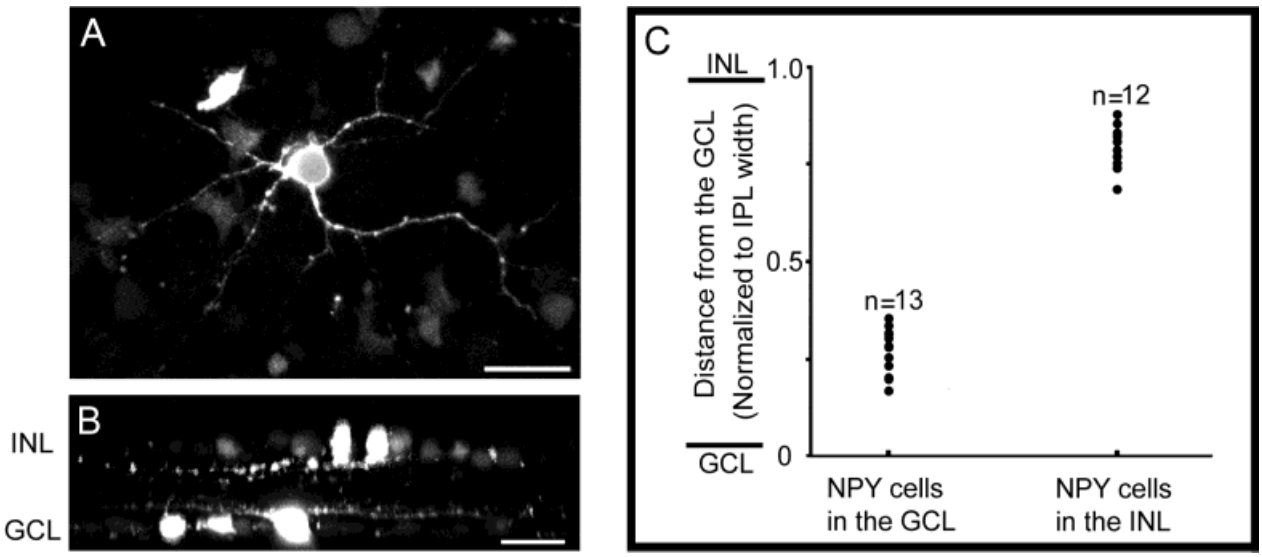

Fig. 7. Location of neuropeptide Y (NPY)/β-gal cell processes in the inner plexiform layer (IPL). Retinal whole-mounts were treated with fluorescein-di-β-D-galactopyranoside (FDG) and imaged by confocal microscopy. The whole-mounts were optically sectioned (in 0.5-μm increments) from the fiber layer through the middle of the inner nuclear layer (INL). **A:** An NPY/β-gal cell labeled with fluorescein using FDG. The cell lies in the ganglion cell layer (GCL) and is viewed from the top. **B:** Side view of several NPY/β-gal cells in both the GCL and INL, showing their ramifications. The image contains two superimposed projections. **C:** Scatter plot showing the normalized distance of the ramifications of 25 cells from the GCL/IPL border. Each cell's ramification was largely or exclusively in one layer (see B). For cells in the GCL, the mean distance was 0.28 ± 0.02 (SEM, n = 13); for cells in INL, the mean distance was 0.80 ± 0.02 (SEM, n = 12). Scale bars = 20 μm in A,B.

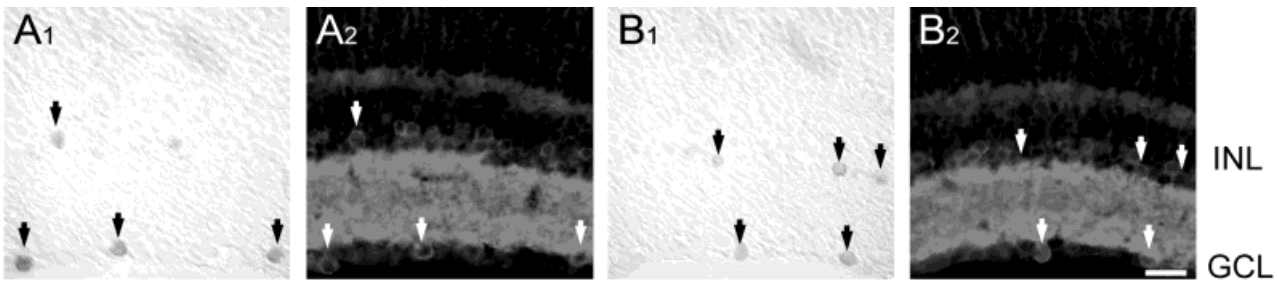

Fig. 8. Neuropeptide Y (NPY)/β-gal cells are immunoreactive for the γ-aminobutyric acid (GABA) transporter, GAT-1. **A_1:** Retinal cross-section (10 μm) stained with Xgal to mark the NPY/β-gal cells. Arrows indicate Xgal-stained cells. **A_2:** Same section labeled with antibodies to GAT-1. Arrows indicate the location of the Xgal-stained cells. **B_1:** A second section stained with Xgal to mark the NPY/β-gal cells. **B_2:** Same section as in B_1 labeled with antibodies to GAT-1. Scale bar = 20 μm in B_2 (applies to A_1–B_2).

NPY cells in the GCL are amacrine cells (Oh et al., 1999) but differ from observations in cat (Hutsler et al., 1993).

NPY immunoreactivity has also been observed in the retinas of nonmammalian species, including turtle (Isayama and Eldred, 1988; Isayama et al., 1988), toad (Zhu and Gibbins, 1995), frog (Bruun et al., 1986), and lizard (Straznicky and Hiscock, 1994). Further variety in the staining patterns is observed when these species are considered. In particular, NPY immunoreactivity in the cane toad retina appears in Muller cells in addition to amacrine cells (Zhu and Gibbins, 1995, 1996), and, in frogs, one population of NPY-IR cells sends processes not just to the IPL but to the OPL (Bruun et al., 1986). Thus, although most species have NPY-IR cells in the innermost row of the INL, many have additional populations, which may play species-specific roles.

Dissecting mouse retinal circuitry

Transgenic techniques provide new ways to perturb retinal processing. Because these techniques are most feasible in the mouse, this species is becoming an attractive choice for studying this processing. Because the mouse retina has not been well-characterized, a valuable first step is to characterize its cell types. In this study, we characterized one biochemically defined population, NPY-expressing cells, and generated predictions about their roles. These cells were described using a transgenic mouse line that expresses β-gal in this population. These predictions can now be tested by removing these cells from the retina by using β-gal–mediated ablation (Nirenberg and Cepko, 1993, Nirenberg and Meister, 1997) and examining the effects on the responses of the ganglion cells.

ACKNOWLEDGEMENTS

We thank John Walsh and Helen Wong for the generous gift of their NPY antibody; Richard Palmiter, Jay Erickson, and Cathy Clegg, for the generous gift of their NPY/β-gal transgenic mouse line; and Kevin Kelley and Karl Herrup for the generous gift of their Thy-1 transgenic mouse line. We also thank Peter Latham for his program for nearest neighbor analysis; Iona D'Angelo and Nick Brecha for advice on NPY immunohistochemistry; and Adam Jacobs, Steve Carcieri, Iona D'Angelo, Larry Kruger, Michael Sofroniew, and John Assad for comments on the manuscript. S.N. received support from the Klingenstein Fund.

LITERATURE CITED

Brecha NC, Weigmann C. 1994. Expression of GAT-1, a high-affinity gamma-aminobutyric acid plasma membrane transporter in the rat retina. J Comp Neurol 345:602–611.

Bonfanti L, Strettoi E, Chierzi S, Cenni MC, Liu XH, Martinou JC, Maffei L, Rabacchi SA. 1996. Protection of retinal ganglion cells from natural and axotomy-induced cell death in neonatal transgenic mice overexpressing bcl-2. J Neurosci 16:4186–4194.

Bruun A, Tornqvist K, Ehinger B. 1986. Neuropeptide Y (NPY) immunoreactive neurons in the retina of different species. Histochemistry 86:135–140.

Cardozo BN, Buijs R, Van Der Want J. 1991. Glutamate-like immunoreactivity in the retinal terminals in the nucleus of the optic tract in rabbits. J Comp Neurol 309:261–270.

Cepko C. 1989. Lineage analysis and immortalization of neural cells via retrovirus vectors. In: Boulton AA, Baker GB, Campagnoni AT, editors. Molecular biological techniques. Clifton, NJ: Humana. p 177–219.

Chen J, Makino CL, Peachey NS, Baylor DA, Simon MI. 1995. Mechanisms of rhodopsin inactivation in vivo as revealed by a COOH-terminal truncation mutant. Science 267:374–377.

Clark PJ, Evans FC. 1954. Distance to nearest neighbor as a measure of spatial relationships in populations. Ecology 35:445–453.

Erickson JC, Clegg KE, Palmiter RD. 1996. Sensitivity to leptin and susceptibility to seizures of mice lacking neuropeptide Y. Nature 381:415–421.

Famiglietti EV Jr, Kolb H. 1976. Structural basis for ON-and OFF-center responses in retinal ganglion cells. Science 194:193–195.

Ferriero DM, Sagar SM. 1989. Development of neuropeptide Y-immunoreactive neurons in the rat retina. Brain Res Dev Brain Res 48:19–26.

He S, Weiler R, Vaney DI. 2000. Endogenous dopaminergic regulation of horizontal cell coupling in the mammalian retina. J Comp Neurol 418:33–40.

Hofbauer A, Drager UC. 1985. Depth-segregation of retinal ganglion cells projecting to the mouse superior colliculus. J Comp Neurol 234:465–474.

Hutsler JJ, Chalupa LM. 1994. Neuropeptide Y immunoreactivity identifies a regularly arrayed group of amacrine cells within the cat retina. J Comp Neurol 346:481–489.

Hutsler JJ, White CA, Chalupa LM. 1993. Neuropeptide Y immunoreactivity identifies a group of gamma-type retinal ganglion cells in the cat. J Comp Neurol 336:468–480.

Isayama T, Eldred WD. 1988. Neuropeptide Y-immunoreactive amacrine cells in the retina of the turtle *Pseudemys scripta elegans*. J Comp Neurol 271:56–66.

Isayama T, Polak J, Eldred WD. 1988. Synaptic analysis of amacrine cells with neuropeptide Y-like immunoreactivity in turtle retina. J Comp Neurol 275:452–459.

Jeon CJ, Strettoi E, Masland RH. 1998. The major cell populations of the mouse retina. J Neurosci 18:8936–8946.

Kelley KA, Friedrich VL Jr, Sonshine A, Hu Y, Lax J, Li J, Drinkwater D, Dressler H, Herrup K. 1994. Expression of Thy-1/lacZ fusion genes in the CNS of transgenic mice. Brain Res Mol Brain Res 24:261–274.

Kolb H, Nelson R, Mariani A.1981. Amacrine cells, bipolar cells and ganglion cells of the cat retina: a Golgi study. Vision Res 21:1081–1114.

Lem J, Krasnoperova NV, Calvert PD, Kosaras B, Cameron DA, Nicolo M, Makino CL, Sidman RL. 1999. Morphological, physiological, and biochemical changes in rhodopsin knockout mice. Proc Natl Acad Sci USA 96:736–741.

MacNeil MA, Masland RH. 1998. Extreme diversity among amacrine cells: implications for function. Neuron 20:971–982.

Main CM, Wilhelm M, Gabriel R. 1993. Colocalization of GABA-immunoreactivity in neuropeptide- and monoamine- containing amacrine cells in the retina of Bufo marinus. Arch Histol Cytol 56:161–166.

Marshak DW. 1989. Peptidergic neurons of the macaque monkey retina. Neurosci Res Suppl 10:S117–S130.

Masland RH. 1988. Amacrine cells. Trends Neurosci 11:405–410.

Masu M, Iwakabe H, Tagawa Y, Miyoshi T, Yamashita M, Fukuda Y, Sasaki H, Hiroi K, Nakamura Y, Shigemoto R. 1995. Specific deficit of the ON response in visual transmission by targeted disruption of the mGluR6 gene. Cell 80:757–765.

McDonald AJ, Pearson JC. 1989. Coexistence of GABA and peptide immunoreactivity in non-pyramidal neurons of the basolateral amygdala. Neurosci Lett 100:53–58.

Nelson R, Famiglietti EV Jr, Kolb H. 1978. Intracellular staining reveals different levels of stratification for on- and off-center ganglion cells in cat retina. J Neurophysiol 41:472–483.

Nirenberg S, Cepko C. 1993. Targeted ablation of diverse cell classes in the nervous system in vivo. J Neurosci 13:3238–3251.

Nirenberg S, Meister M. 1997. The light response of retinal ganglion cells is truncated by a displaced amacrine circuit. Neuron 18:637–650.

Oh SJ, Kim IB, Lee EJ, Brecha N, Chun MH. 1999. Morphology and synaptic connectivity of neuropeptide Y immunoreactive neurons in the rat retina. Invest Opthalmol Vis Sci 40:S439.

Peichl L, Wassle H. 1981. Morphological identification of on- and off-centre brisk transient (Y) cells in the cat retina. Proc R Soc Lond B Biol Sci 212:139–153.

Perry VH, Walker M. 1980. Amacrine cells, displaced amacrine cells and interplexiform cells in the retina of the rat. Proc R Soc Lond B Biol Sci 208:415–431.

Sandell JH, Masland RH. 1986. A system of indoleamine-accumulating neurons in the rabbit retina. J Neurosci 6:3331–3347.

Soucy E, Wang Y, Nirenberg S, Nathans J, Meister M. 1998. A novel signaling pathway from rod photoreceptors to ganglion cells in mammalian retina. Neuron 21:481–493.

Straznicky C, Hiscock J. 1989. Neuropeptide Y-like immunoreactivity in neurons of the human retina. Vision Res 29:1041–1048.

Straznicky C, Hiscock J. 1994. Neuropeptide Y-immunoreactive neurons in the retina of two Australian lizards. Arch Histol Cytol 57:151–160.

Toda K, Bush RA, Humphries P, Sieving PA. 1999. The electroretinogram of the rhodopsin knockout mouse. Vis Neurosci 16:391–398.

Tornqvist K, Ehinger B. 1988. Peptide immunoreactive neurons in the human retina. Invest Ophthalmol Vis Sci 29:680–686.

Vaney DI. 1990. The mosaic of amacrine cells in the mammalian retina. In: Osborne NN, Chader C, editors. Progress in retinal research. Oxford, UK: Pergamon. p 49–100.

Vaney DI, Peichi L, Boycott BB. 1981. Matching populations of amacrine cells in the inner nuclear and ganglion cell layers of the rabbit retina. J Comp Neurol 199:373–391.

Wassle H, Riemann HJ. 1978. The mosaic of nerve cells in the mammalian retina. Proc R Soc Lond B Biol Sci 200:441–461.

Xu J, Dodd RL, Makino CL, Simon MI, Baylor DA, Chen J. 1997. Prolonged photoresponses in transgenic mouse rods lacking arrestin. Nature 389: 505–509.

Yang RB, Robinson SW, Xiong WH, Yau KW, Birch DG, Garbers DL. 1999. Disruption of a retinal guanylyl cyclase gene leads to cone-specific dystrophy and paradoxical rod behavior. J Neurosci 19:5889–5897.

Zhu BS, Gibbins I. 1995. Synaptic circuitry of neuropeptide-containing amacrine cells in the retina of the cane toad, *Bufo marinus*. Vis Neurosci 12:919–927.

Zhu BS, Gibbins I. 1996. Muller cells in the retina of the cane toad, *Bufo marinus*, express neuropeptide Y-like immunoreactivity. Vis Neurosci 13:501–508.